

The Quantum Pinch Effect in Semiconducting Quantum Wires: A Bird's-Eye View

Manvir S. Kushwaha

Department of Physics and Astronomy, Rice University, P.O. Box 1892, Houston, TX 77251, USA

(Dated: September 1, 2016)

Abstract

Those who measure success with culmination do not seem to be aware that life is a journey not a destination. This spirit is best reflected in the unceasing failures in efforts for solving the problem of controlled thermonuclear fusion for even the simplest pinches for over decades; and the nature keeps us challenging with examples. However, these efforts have permitted researchers the obtention of a dense plasma with a lifetime that, albeit short, is sufficient to study the physics of the pinch effect, to create methods of plasma diagnostics, and to develop a modern theory of plasma processes. Most importantly, they have impregnated the solid state plasmas, particularly the electron-hole plasmas in semiconductors, which do not suffer from the issues related with the confinement and which have demonstrated their potential not only for the fundamental physics but also for the device physics. Here, we report on a two-component, cylindrical, quasi-one-dimensional quantum plasma subjected to a *radial* confining harmonic potential and an applied magnetic field in the symmetric gauge. It is demonstrated that such a system as can be realized in semiconducting quantum wires offers an excellent medium for observing the quantum pinch effect at low temperatures. An exact analytical solution of the problem allows us to make significant observations: surprisingly, in contrast to the classical pinch effect, the particle density as well as the current density display a *determinable* maximum before attaining a minimum at the surface of the quantum wire. The effect will persist as long as the equilibrium pair density is sustained. Therefore, the technological promise that emerges is the route to the precise electronic devices that will control the particle beams at the nanoscale.

PACS numbers: 73.63.Nm, 52.55.Ez, 52.58.Lq, 85.35.Be

Keywords: Quantum wires, magneto-transport, nanoscale devices, pinch effect, self-focusing

I. A KIND OF INTRODUCTION

The greatest scientific challenge in the history of civilization is known to be set forth with ancient belief in the five *basic* elements: earth, water, air, fire, and aether [see, e.g., the Yoonir in Fig. 1]. Early credence in these basic elements dates back to pre-Socratic times and persisted throughout the Middle Ages and into the Renaissance, deeply influencing European thought and culture. These five elements are also sometimes associated with the five platonic solids. Many philosophies have a set of five elements believed to reflect the simplest essential principles upon which the constitution of everything is based. Most frequently, five elements refer to the ancient concepts which some science writers compare to the present-day states of matter, relating earth to solid, water to liquid, air to gas, and fire to *plasma*. Historians trace the evolution of modern theory of chemical elements, as well as chemical compounds, to medieval and Greek models. According to Hinduism, the five elements are found in *Vedas*, especially *Ayurveda*; are associated with the five senses: (i) hearing, (ii) touch, (iii) sight, (iv) taste, and (v) smell; and act as the gross medium for the experience of sensations. They further suggest that all of creation, including the human body, is made up of these five elements and that, upon death, the human body dissolves into these five elements, thereby balancing the divine cycle of nature.

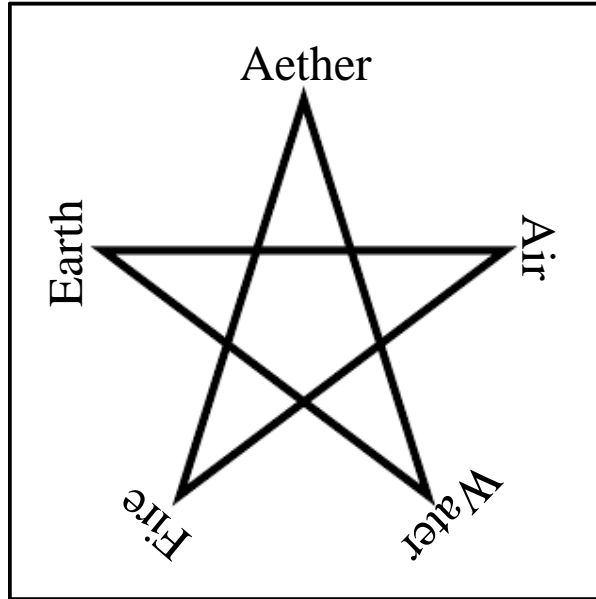


FIG. 1: (Color online) The Yoonir [or, more formally, the Star of Yoonir] is one of the most important and sacred cosmological symbols in the Serer religion. It is the brightest star of the universe and commonly known as the Star of Sirius. Because of its uniqueness, I choose it to represent the five *basic* elements of life.

This review article has very much to do with the plasma – another ghostly gift of Mother Nature – a state of matter whose size and/or shape is beyond imagination. A plasma is, by definition, an ionized gas in which the length which separates the single-particle behavior from the collective behavior is smaller

than the characteristic lengths of interest. Researchers in plasma physics have come to the recognition that 99.999% of the mass of the universe exists in the form of plasma. The term plasma refers to the *blood* of the universe. Plasma is invisible; pervades all space in gigantic streams; powers everything; every galaxy, every star; formed by the nature of its dynamics; and its organization in space is shaped by the electromagnetic force of the universe. The same force also pinches the streams ever tighter, until the concentration becomes so great that *explosive* node-points result where plasma dissipates. Our Sun is known to be located at the center of one of the node points [see Fig. 2]. Physically, plasma is loosely defined as globally neutral medium made up of unbound electrically charged particles. The term unbound, by no means, refers to the particles being free from experiencing forces. When the charges move, they generate electric currents which create magnetic fields which, in turn, act upon the currents and, as a result, they are affected by each others fields. Much of the understanding of plasmas has come from the pursuit of controlled nuclear fusion and fusion power, for which plasma physics provides the scientific basis. As to the interpretation of (space) plasma dynamics, the magnetohydrodynamics (MHD) that provides theoretical framework has always stood to the test.

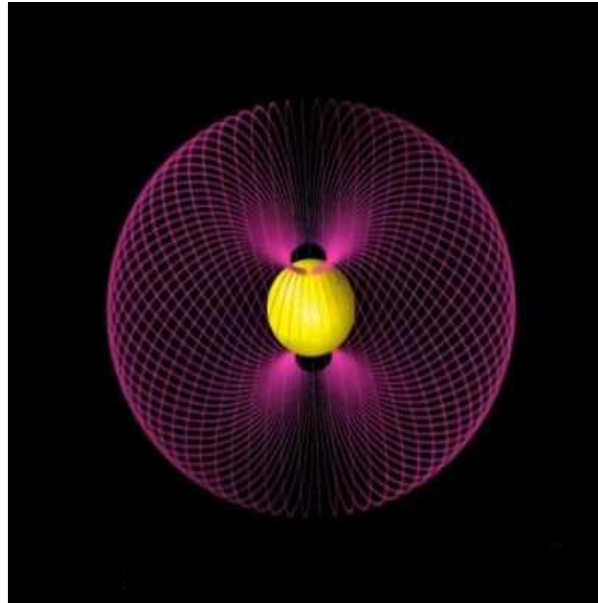


FIG. 2: (Color online) The geometry of the Sun at a plasma node. At this point on, plasma expands again and moves on, collecting more plasma as it flows around in the space. Instead of plasma exploding at the node point of the Sun, the Sun consumes the plasma... [After the Home page of Rolf A. Witzsche.]

Literature is a live witness that pinches were the first device used by mankind for controlled nuclear fusion. *Pinch effect is the manifestation of self-constriction of plasma caused by the action of a magnetic field that is generated by the parallel electric currents.* The result of this manifestation is that the plasma is heated as well as confined. The phenomenon is also referred to as Bennett pinch, electro-

magnetic pinch, plasma pinch, magnetic pinch, or (most commonly) the pinch effect. Pinch effect takes place naturally in electrical discharges such as lightning bolts [see, e.g., Fig. 3], the auroras, current sheets, and solar flares. Pinches may become unstable. They radiate energy as light across the whole electromagnetic spectrum including x-rays, radio waves, gamma rays, synchrotron radiation, and visible light. They also produce neutrons, as a result of fusion – although a desired nuclear fusion has never been achieved because the confinement and the instability are two concurrent and diametric events. As to the applications, pinches are used to generate x-rays and the intense magnetic fields generated are used in forming of the metals [see, e.g., Fig. 4]. They also have applications in astrophysical studies, space propulsion, and particle beam weapons. Numerous large pinch machines have been built in order to study the fusion power. Clearly, a cylindrical geometry is pertinent to the effect.



FIG. 3: (Color online) Lightning bolts illustrating electromagnetically pinched plasma filaments is an example of plasma present at Earth’s surface. Typically, lightning discharges 30,000 amperes at up to 100 million volts, and emits light, radio waves, X-rays and even gamma rays. Plasma temperatures in lightning can approach 28,000 K (28,000 C; 50,000 F) and electron densities may exceed 10^{24} m^{-3} . [Courtesy of the Wikipedia].

The magnetic self-constriction (or self-attraction) of the parallel electric currents is the best-known and the simplest example of Ampère’s force law, which states that the force per unit length between two straight, parallel, conducting wires is given by

$$\frac{F_m}{L} = 2k_A \frac{I_1 I_2}{r}, \quad (1)$$

where k_A is the magnetic force constant from the Biot-Savart law, F_m/L is the total force on either wire per unit length (of the shorter), r is the distance between the two wires, and I_1, I_2 are the direct currents carried by the wires. This is a good approximation if one wire is sufficiently longer than the other that

it can be approximated as infinitely long, and if the distance between the wires is small compared to their lengths (so that the one infinite-wire approximation holds), but large compared to their diameters (so that they may also be approximated as infinitely thin lines). The value of k_A depends upon the system of units chosen and decides how large the unit of current will be. In the SI system, $k_A = \mu_0/4\pi$, with $\mu_0 = 4\pi \times 10^{-7} \text{ N/A}^2$; whereas in the CGS system, $k_A = 1$. For the modest current levels of a few amperes, this force is usually negligible, but when current levels approach a million amperes, such as in electrochemistry, this force can be significant since the pressure is proportional to I^2 . The form of Ampère's force law commonly given was derived by Maxwell and is one of the several expressions consistent with the original experiments of Ampère and Gauss. Note in passing that the Ampère's law underlies the definition of the ampere, the SI unit of current.



FIG. 4: (Color online) Electromagnetically pinched aluminium can, produced from a pulsed magnetic field created by rapidly discharging 2 kilojoules from a high voltage capacitor bank into a 3-turn coil of heavy gauge wire. [After Bert Hickman, Stoneridge Engineering].

Let us scrutinize how and why the pinch effect comes into being. For this purpose, we consider a cylindrical coordinate frame with the axis z along the axis of the wire. For the moment, we do not even need to know its size such as the radius. We assume that the electrons (of charge $-e$, with $e > 0$) flow in the positive direction of the z axis with a velocity $\mathbf{v} > 0$. For the symmetry reasons, we restrict the magnetic field to be azimuthal, i.e., to have only component $B_\theta = B_\theta(r)$. In order to evaluate B_θ , we use Ampere's law in the integral form for the circular path as depicted in Fig. 5. The result is that $B_\theta = (2\pi r/c) J$, where $J = -n_e e v < 0$. Therefore, $B_\theta < 0$, i.e., it is oriented clockwise with respect to the z axis. The magnetic force $\mathbf{F} = -(e/c)(\mathbf{v} \times \mathbf{B}) = -2\pi n_e e^2 (v^2/c^2) \mathbf{r}$ is in the radial direction guided

towards the axis. The dependence on e^2 implies that the force is independent of the sign of the charge. Clearly then, the magnetic force tends to push the electrons towards the axis of the wire. In other words, in a flowing current beam the self-generated magnetic field always acts to *pinch* the beam – or to let it shrink around the axis. Next, the Lorentz force $\mathbf{F} = -e(\mathbf{E} + (1/c)(\mathbf{v} \times \mathbf{B}))$ yields $\mathbf{E} = -(1/c)(\mathbf{v} \times \mathbf{B})$ for \mathbf{F} to be zero. This yields $\mathbf{E} = -2\pi n_e e(v^2/c^2)\mathbf{r}$. From the integral form of the Gauss theorem, we find that this field is generated by a charge density ρ , which is uniform over the wire such that $E = 2\pi r\rho$, which gives $\rho = -n_e e(v^2/c^2)$. Since $\rho = e(n_i - n_e)$ holds, we obtain $n_e = n_i/[1 - v^2/c^2]$; n_i being the ion density. The electron density is uniform, but it exceeds the value $n_e = n_i$ that would ensure $\rho = 0$. This leads us to infer that there has been some accumulation of electrons inside the wire, rising the density by a factor $(1 - v^2/c^2)$. For an electron in an Ohmic conductor usually $v \approx 1$ cm/sec, thus $v^2/c^2 \approx 10^{-20}$ implying that the pinch effect is too small to be observed. The effect can be robust in high density particle beam or plasma columns where v/c is non-negligible.

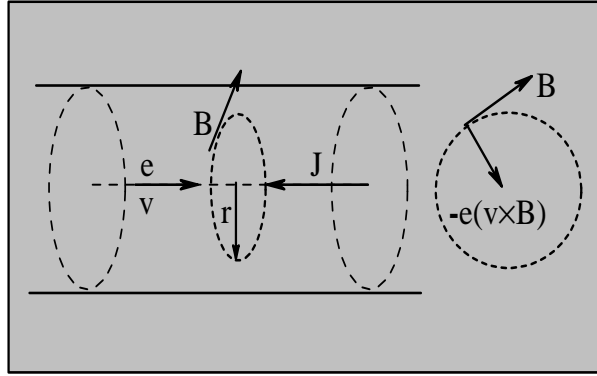


FIG. 5: (Color online) A cylindrical geometry utilized to demonstrate how and why the pinch effect is [and can be] a real deal given the appropriate plasma medium where v^2/c^2 is not much less than one.

Characteristically, the pinch effect can be understood most easily through the example of a current flowing along the axis of a cylinder filled with a conducting medium. The lines of force of the magnetic field \mathbf{B} generated by the current have the form of the concentric circles whose planes are perpendicular to the axis of the cylinder. The electrodynamic force per unit volume of a conducting medium with a current density \mathbf{J} is $\mathbf{F} = (1/c)(\mathbf{J} \times \mathbf{B})$; this force is guided towards the axis of the cylinder and tends to squeeze down the medium. The state that arises is the pinch effect. The pinch effect may also be considered a simple consequence of Ampere's law [see above], which describes the magnetic attraction between the individual parallel current filaments whose aggregate is the current cylinder. Notice that the magnetic pressure (P_m) is impeded by the kinetic pressure (P_k) – directed from the axis – of the medium arising from the thermal motion of the medium's particles. When the current is sufficiently large such that the *plasma* $\beta [= P_k/P_m] < 1$, the pinch effect comes into being. The pinch effect

requires that the population of the charge carriers of opposite signs in the medium be nearly equal. In a medium of charge carriers of single sign, the electric field of the space charge effectively impedes the inward action of the magnetic pressure. It is obvious by now that the pinch effect is paramount in the problems of controlled thermonuclear fusion. As to the geometries [see Appendix A], the term θ -pinch has come into wide usage to denote an important confinement scheme which relies on the repulsion of oppositely directed currents and which is thus not in accord with the original definition of the pinch effect – self-attraction of the parallel currents. As such, the z-pinch remains by far the most preferred scheme for the plasma confinement [see Fig. 6].

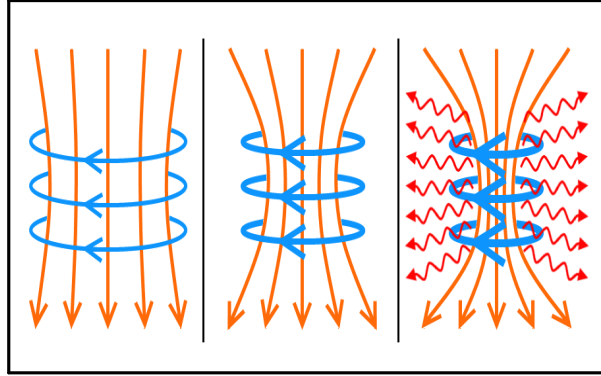


FIG. 6: (Color online) Schematics of the Z-pinch: A current (orange) generates a magnetic field (blue), which causes the current to pinch inwards along the axis by way of the Biot-Savart force: $\mathbf{F} = (1/c)(\mathbf{J} \times \mathbf{B})$. This amplifies the magnetic field and accelerates the pinch, heating the plasma and causing it to radiate X-rays (red).

In order to take this brief history of the pinch effect to the point where it was formally discussed first, we would like to recall the mechanism behind the Bennett pinch in the gaseous plasmas. Incidentally, the Bennett pinch is also known by other names such as equilibrium or steady-state pinch because in the Bennett pinch no variable is a function of time. As stated above, while the magnetic pressure tends to confine the plasma, the kinetic pressure tends to oppose it. When these forces are balanced, an equilibrium is attained. The resulting state is what we call the Bennett pinch. Therefore, the use of the steady-state MHD model in which $\nabla p = (1/c)(\mathbf{J} \times \mathbf{B})$ makes sense. Here $p = nk_B(T_e + T_i)$ is the kinetic pressure of the plasma particles due to its thermal motion – as a reaction to the magnetic force. Symbols $n = (n_e = n_i)$, k_B , and T_e (T_i) are, respectively, the particle density, Boltzmann's constant, and electron (ion) temperature. Notice that p , \mathbf{J} , and \mathbf{B} are all local (r -dependent) functions. The equilibrium z-pinch can be described by the balance of kinetic pressure at the axis and magnetic pressure at the surface ($r = a$):

$$n k_B (T_e + T_i) = -\frac{B_\theta^2(a)}{8\pi}. \quad (2)$$

The magnetic field at the cylindrical surface is calculated from the total current by using the Ampère's

law to write

$$B_{\theta}(a) = \frac{2I}{ca}. \quad (3)$$

These two equations allow us to determine the relationship between the pinch radius, the temperature at the axis, and the total current:

$$(T_e + T_i) \propto \frac{I^2}{a^2}. \quad (4)$$

This is known as the Bennett-relation after Willard H. Bennett who first discussed this z-pinch effect in 1934. Equation (4) estimates the total current that must be discharged through the plasma medium in order to confine the plasma at a specified temperature for a given linear particle density and the pinch radius a . Figure 7 illustrates his typical chart showing the total current (I) versus the number of particles per unit length (N) in four distinct regimes. The conducting medium is plasma which is assumed to be non-rotational and P_k at the surface is much smaller than near the axis.

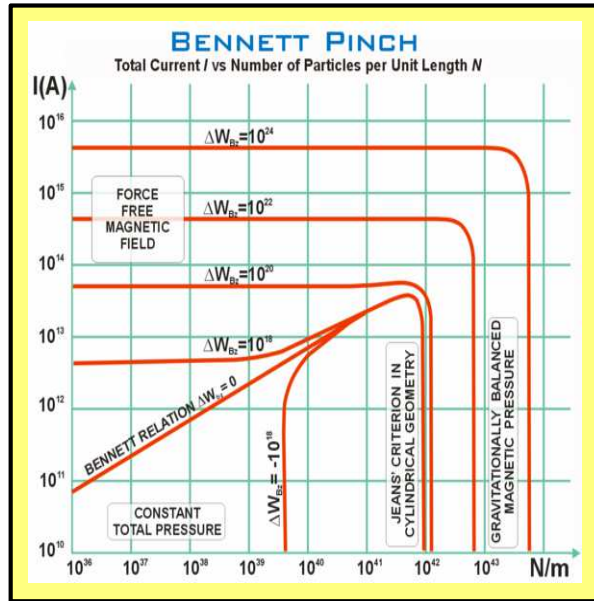


FIG. 7: (Color online) The static Z-pinch showing the total current (I) versus the number of particles per unit length (N) – first studied by Bennett in 1934. The chart illustrates four physically distinct regions. The plasma temperature is 20 K, the mean particle mass 3×10^{-27} kg, and $\Delta W B_z$ is the excess magnetic energy per unit length due to the axial magnetic field B_z . The plasma is assumed to be non-rotational, and the kinetic pressure at the edges is much smaller than inside. [Courtesy of the Wikipedia].

II. THE QUANTUM PINCH EFFECT IN QUANTUM WIRES

The pinch effect is one of the most fascinating phenomena in plasma physics with immense applications to the problems of peace and war. It is the manifestation of radial constriction of a compressible conducting plasma [or a beam of charged particles] due to the magnetic field generated by the parallel electric currents. Cylindrical symmetry is central to the realization of the effect. In the literature, the phenomenon is also referred to as self-focusing, magnetic pinch, plasma pinch, or Bennett pinch. The pinch effect in the cylindrical geometry is classified after the direction in which the current flows: In a θ -pinch, the current is azimuthal and the magnetic field axial; in a z -pinch, the current is axial and the magnetic field azimuthal; in a screw (or θ - z) pinch, an effort is made to combine both θ -pinch and z -pinch [see Fig. 8 and Appendix A].

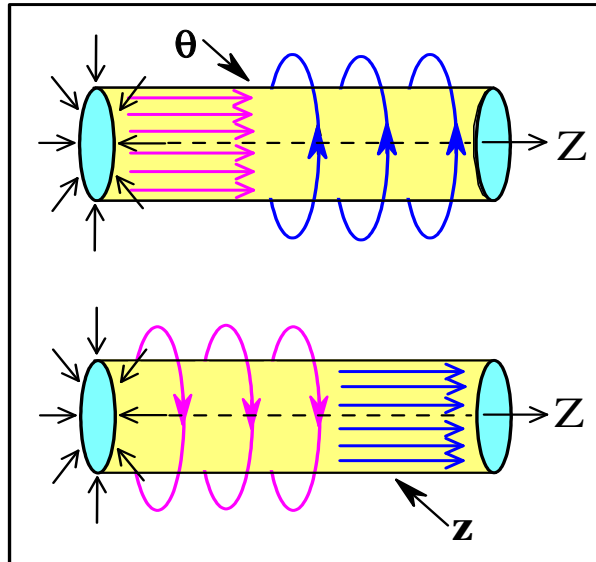


FIG. 8: (Color online) The schematics of the θ -pinch (the upper panel) and the z -pinch (the lower panel). The curves in blue (magenta) refer to the current (magnetic field). [After Kushwaha, Ref. 39].

While a popular reference dates back to 1790 when Martinus van Marum in Holland created an explosion by discharging 100 Leyden jars into a wire, the first formal study of the effect was not undertaken until 1905 when Pollock and Barraclough [1] investigated a compressed and distorted copper tube after it had been struck by lightning [see Fig. 9]. They argued that the magnetic forces due to the large current flow could have caused the compression and distortion. Shortly thereafter, Northrup published a similar but independent diagnosis of the phenomenon in liquid metals [2]. However, the major breakthrough in the topic came with the publication of the derivation of the radial pressure balance in a static z -pinch by Bennett [3]. Curiously enough, the term “pinch effect” was only coined in 1937 by Tonks in his work on the high current densities in low pressure arcs [4]. This was followed by

a *first* patent for a fusion reactor based on a toroidal z-pinch submitted by Thompson and Blackman [5]. The subsequent progress – theoretical and experimental – on the pinch effect in the gas discharges was driven by the quest for the controlled nuclear fusion.

Needless to say, the plasma commands a glamorous status in the physics literature by representing the *fourth* state of matter. Our key interest here is in the solid state plasmas (SSP), which share several characteristic features with but are also known to have quantitative differences from the gaseous space plasmas (GSP). The GSP is ill-famed for two inherently juxtaposing characteristics: confinement and instability. The SSP is, on the contrary, a uniform, equilibrium system tightly bound to the lattice where the boundary conditions make no sense, whereas in GSP they can be crucial. Notice that only two-component, semiconductor SSP with approximately equal number of electrons and holes can support a significant pinching. For a single mobile carrier the space-charge electric field due to any alteration in the charge-density will impede such inward motion. Thus a metal with only electrons contributing to the conduction is a poor option. The 1960's had seen considerable experimental [6-15] and theoretical [16-19] efforts focused on studying pinch effect in the bulk SSP, with instabilities manifesting themselves as voltage and current oscillations at frequencies up to 50 MHz.

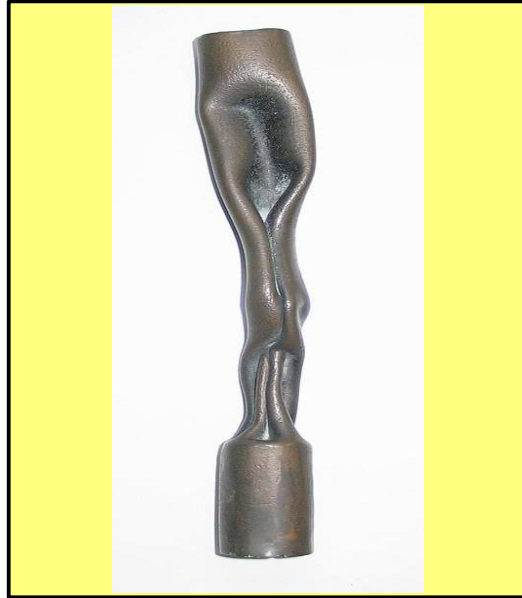


FIG. 9: (Color online) A photograph of a section of the crushed copper tube from a lightning rod first described by Pollock and Barraclough (1905). They correctly described the crushing mechanism as a result of the interaction of the large current flowing in the conductor with its own magnetic field. [Courtesy of the Wikipedia].

Notwithstanding the SSP had been imbued to a greater extent by the research pursuit for the pinch effect in the GSP, the subject did not gain sufficient momentum because the early 1970's had begun to offer the condensed matter physicists with the new venues to explore: the semiconducting

quantum structures with reduced dimensions such as quantum wells, quantum wires, quantum dots, and their periodic counterparts. The continued tremendous research interest in these quasi-n-dimensional electron gas [Q-nDEG] systems can now safely be accredited to the discovery of the quantum Hall effects – both integral [20] and fractional [21]. The fundamental issue behind the excitement in these man-made nanostructures lies in the fact that the charge carriers exposed to external probes such as electric and/or magnetic fields can exhibit unprecedented quantal effects that strongly modify their behavior characteristics [22-38]. To what extent these effects can influence the behavior of a quantum wire [or, more realistically, Q-1DEG system] in the cylindrical symmetry, which offers a quantum analogue of the classical structure subjected to investigate the pinch effect in the conventional SSP [or GSP], has not yet been explored. This was the motivation behind the original work on the quantum pinch effect investigated in semiconducting quantum wires in Ref. 39.

We consider a two-component, quasi-1DEG system characterized by a radial harmonic confining potential and subjected to an applied (azimuthal and axial) magnetic field in the cylindrical symmetry. The two-component Q-1DEG systems are comprised of both types of charge carriers [i.e., electrons and holes] and are known to have been fabricated in a wide variety of semiconducting quantum wires by optical pumping techniques [40-42]. In the linear response theory, the resultant system is characterized by the single-particle Hamiltonian $H = H_0 + H_1$, where [after Peierls substitution $\mathbf{p} \rightarrow (\mathbf{p} \pm \frac{e}{c}\mathbf{A})$, with $\mathbf{A} = \mathbf{A}_0 + \mathbf{A}_1$]

$$H_0 = \frac{1}{2}m_e\mathbf{v}_e^2 + \frac{1}{2}m_h\mathbf{v}_h^2 + \frac{1}{2}m_e\omega_e^2r^2 + \frac{1}{2}m_h\omega_h^2r^2, \quad (5)$$

$$H_1 = \frac{e}{2c}[(\mathbf{v}_e \cdot \mathbf{A}_1 + \mathbf{A}_1 \cdot \mathbf{v}_e) - (\mathbf{v}_h \cdot \mathbf{A}_1 + \mathbf{A}_1 \cdot \mathbf{v}_h)], \quad (6)$$

to first order in \mathbf{A}_1 , where \mathbf{A}_0 (\mathbf{A}_1) is the *dc* (*ac*) part of the vector potential \mathbf{A} . Here c is the speed of light in vacuum and $-e(+e)$, $m_e(m_h)$, and $\omega_e(\omega_h)$ are, respectively, the electron (hole) charge, mass, and the characteristic frequency of the harmonic oscillator. $\mathbf{v}_i = \frac{1}{m_i}(\mathbf{p} \pm \frac{e}{c}\mathbf{A}_0)$ is the velocity operator for an electron (hole). A few significant aspects of the formalism are: (i) the formal Peierls substitution, by which a magnetic field is introduced into the Hamiltonian, is a direct consequence of gauge invariance under the transformation $\psi \rightarrow \psi e^{i\phi}$, with ϕ being an arbitrary phase, (ii) in the Coulomb gauge $\nabla \cdot \mathbf{A} = 0 \Rightarrow \mathbf{A} \cdot \mathbf{p} = \mathbf{p} \cdot \mathbf{A}$, and (iii) we choose symmetric gauge, which is quite popular in the many-body theory, defined by $\mathbf{A}_0 = B(0, \frac{1}{2}r, 0)$.

Next, we consider, for the sake of simplicity, the quantization energy for the electrons equal to that for the holes implying that $\omega_e = \omega_o = \omega_h$. Then, in the cylindrical coordinates $[(r, \theta, z)]$, the Schrödinger equation $H_0\psi = \epsilon\psi$ for a quantum wire of radius R and length L is solved to characterize the system

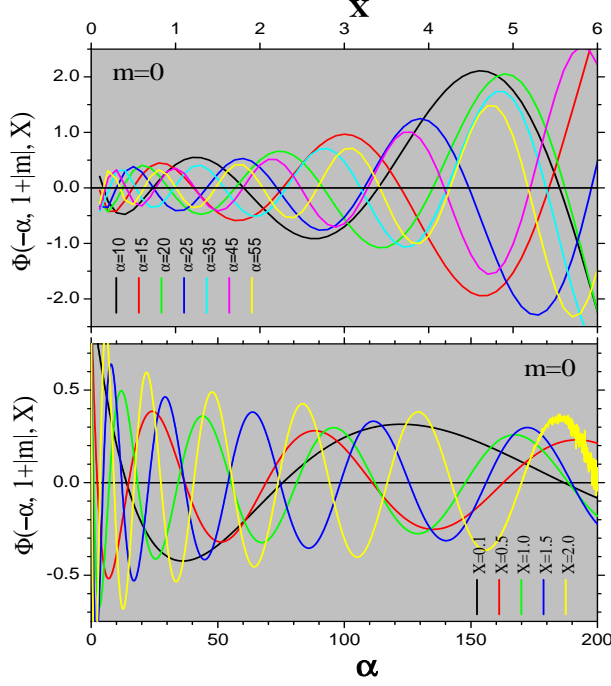


FIG. 10: (Color online) The plot of the CHF $\Phi(\alpha, 1 + |m|, X)$ vs. X (the upper panel) and α (the lower panel), for $m = 0$. [After Kushwaha, Ref. 39].

with the eigenfunction $\psi(r, \theta, z) = \psi(r) \psi(\theta) \psi(z)$, where

$$\psi(z) = \sqrt{\frac{2}{L}} \sin(kz), \quad \text{with } k = n\pi/L, \quad (7)$$

$$\psi(\theta) = \sqrt{\frac{1}{2\pi}} e^{im\theta}, \quad (8)$$

$$\psi(r) = \frac{N}{s^{|m|/2}} e^{-X/2} X^{|m|/2} \Phi(-\alpha; 1 + |m|; X), \quad (9)$$

where n is an integer, $m = 0, \pm 1, \pm 2, \dots$ is the azimuthal quantum number, $s = \sqrt{m_+/\mu}$, and $X = r^2/(2\ell_c^2)$, with $\ell_c = \sqrt{\hbar/\mu\Omega_+}$ as the effective magnetic length in the problem, $m_+ = m_e + m_h$ as the total mass, $\mu = m_e m_h / (m_e + m_h)$ as the reduced mass, $\Omega_+ = s\Omega = s\sqrt{\omega_{ce}\omega_{ch} + 4\omega_o^2}$ as the effective hybrid frequency, and $\omega_{ci} = eB/(m_i c)$ as the cyclotron frequency. In Eq. (9), N is the normalization coefficient to be determined by the condition $\int_0^R dr r |\psi(\dots)|^2 = 1$, which yields

$$N^{-2} = \frac{\ell_c^2}{s^{|m|}} \int_0^\zeta dX e^{-X} X^{|m|} [\Phi(-\alpha; 1 + |m|; X)]^2 \quad (10)$$

where the upper limit $\zeta = R^2/2\ell_c^2$. In Eq. (9), $\Phi(-\alpha; 1 + |m|; X)$ is the confluent hypergeometric function (CHF) [43-45], which is a solution of the Kummer's equation: $XU'' + [1 + |m| - X]U' + \alpha U = 0$, where $\alpha = \frac{1}{\hbar\Omega_+} [\epsilon - \frac{\hbar^2 k^2}{2\mu} - \frac{m}{2} \hbar\Omega_-] - \frac{1}{2}(1 + |m|)$, with $\Omega_- = (\omega_{ce} - \omega_{ch})$ being the effective cyclotron frequency. The wavefunction $\psi(\dots)$ obeys the boundary condition $\psi(r = R) = 0 \Rightarrow \Phi(-\alpha; 1 + |m|; \zeta) = 0$, which

yields

$$\frac{\epsilon'}{\epsilon_r} = \zeta \left[\alpha + \frac{1}{2} \left(1 + m \frac{\Omega_-}{\Omega_+} + |m| \right) \right] \quad (11)$$

where $\epsilon' = \epsilon - \frac{\hbar^2 k^2}{2\mu}$ and $\epsilon_r = 2\hbar^2/(\mu R^2)$. It should be pointed out that the term $\frac{\hbar^2 k^2}{2\mu}$ is only additive and hence inconsequential. What is important to notice though is that, for a given m , ζ and α are determined self-consistently where $\Phi(-\alpha; 1 + |m|; X) = 0$. Figure 10 demonstrates that $\Phi(\dots)$ is unambiguously a well-behaved function over a wide range of X and α and that its period is seen to be decreasing with increasing X or α as the case may be. Since the rest of the illustrative examples require the quantum wire to be specified, we choose GaAs/Ga_{1-x}Al_xAs system: $m_e = 0.067m_0$, $m_h = 0.47m_0$, and the aspect ratio $r_a = L/R = 10^3$ [46]. Another important parameter in the problem is the reduced magnetic flux ϕ/ϕ_0 : the ratio of the magnetic flux [$\phi = B\pi R^2$] to the quantum flux [$\phi_0 = hc/e$] – yielding $\phi/\phi_0 = \zeta$.

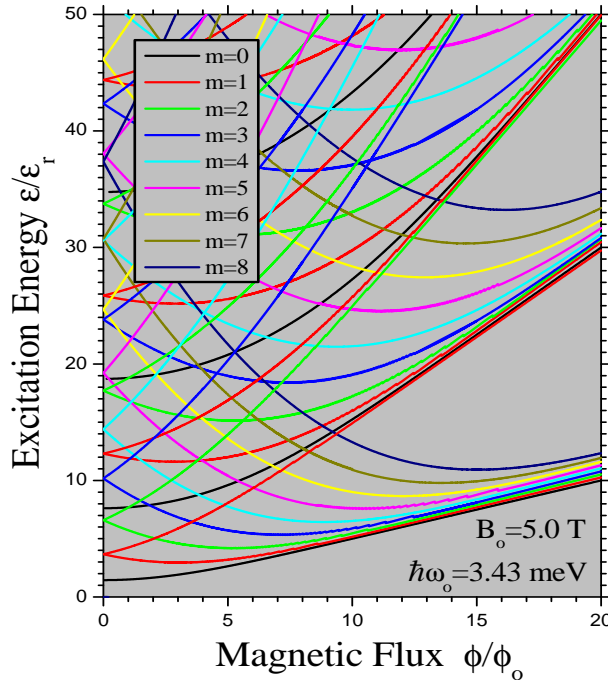


FIG. 11: (Color online) The excitation spectrum for a (finite) cylindrical quantum wire subjected to a magnetic field in the symmetric gauge. The y (x) axis refers to the reduced energy (reduced magnetic flux). The lower (upper) arm of a wedge corresponds to a negative (positive) value of m . [After Kushwaha, Ref. 39].

Figure 11 illustrates the excitation spectrum for the cylindrical quantum wire of finite length as a function of the reduced magnetic flux ϕ/ϕ_0 , for several values of m . This is a result of (involved) computation based on Eq. (11) within the strategy as stated above. The parameters used are as listed inside the picture. For every m , the lower (upper) branch of the wedge corresponds to the negative (positive) value of m . It is interesting to see that both arms of each wedge gradually approach the

Landau levels at higher magnetic flux, just as in the case of the Fock-Darwin spectrum of a quantum dot [see, e.g., Ref. 24]. Notice that this is not a mere coincidence, rather a consequence of the isomorphism in the expression of the single-particle energies for the two quantum systems.

Next, we proceed to the evaluation of the electrical current density \mathbf{J} derived as [with $m_e < m_h$]

$$\mathbf{J} = \frac{ie\hbar}{2m_e} (\psi \nabla \psi^* - \psi^* \nabla \psi) + \frac{e^2}{m_e c} \mathbf{A} \psi^* \psi, \quad (12)$$

where the vector potential \mathbf{A} is approximated such that we seek to measure its *ac* part (\mathbf{A}_1) just as we do its *dc* one (\mathbf{A}_0), i.e., we express \mathbf{A}_0 in the symmetric gauge just as before and $\mathbf{A}_1 = B(0, 0, r)$. This is not to say that there aren't other, more subtle, ways to complicate the situation, but since this is the first paper of its kind, we choose to stick to the bare-bone simplicity – the complexity will (and should) come later. Consequently, it is not difficult to split Eq. (12) into its scalar components:

$$\begin{aligned} J_\theta &= \left[\frac{e\hbar m}{m_e r} + \frac{e^2 B r}{2sm_e} \right] |\psi(r, \theta, z)|^2 \\ J_z &= \frac{e^2 B r}{sm_e} |\psi(r, \theta, z)|^2. \end{aligned} \quad (13)$$

The very nature of the magnetic field – with its charismatic role in localizing the charge carriers in the plane perpendicular to its orientation – elucidates why the radial component of the current density $J_r = 0$. It is interesting to notice that in the absence of the z component of \mathbf{A}_1 , J_z will be zero for a quantum wire of *finite* length (as is the case here). This is contrary to the case of a wire of an *infinite* length – where $J_z \neq 0$ even when $[\mathbf{A}_1]_z = 0$. Equations (13) should, in principle, provide the clue to the quest in the problem.

Figure 12 shows the 1D particle density (n_{1D}) in the quantum wire as a function of the reduced radius for various values of the magnetic field (left panel) and confinement potential (right panel). The confinement potential in the left panel is $\hbar\omega_0 = 1.0$ meV and the magnetic field in the right panel is $B = 1.0$ T. The Other parameters are listed inside the picture. The particle density shows a maximum. We were able to find out that this maximum occurs unequivocally at $\frac{d}{dr}[n_{1D}] = \frac{d}{dr}[r\Phi^2(\alpha, 1+|m|, X)] = 0 \Rightarrow r/R = 1/\sqrt{2\zeta} = 0.3271$. Since the particle density is fundamental to most of the electronic, optical, and transport properties, we expect the current features to make a mark in those phenomena, at least, in the cylindrical symmetry. In a quantum system the particle density has much to do with the Fermi energy in the system. For the fact that each quantum level can take two electrons with opposite spin, the Fermi energy ϵ_F of a system of \mathcal{N} noninteracting electrons for a *finite* system at absolute zero temperature is equal to the energy of the $\frac{1}{2}\mathcal{N}$ -th level. As such, one can compute self-consistently the Fermi energy in a *finite* quantum wire containing \mathcal{N} electrons through this expression: $\mathcal{N} = 2 \sum_m \theta(\epsilon_F - \epsilon'_m)$, where $\theta(\dots)$ is the Heaviside step function and the summation is only over the azimuthal quantum number m . The prime on ϵ_m has the same meaning as explained before. Because

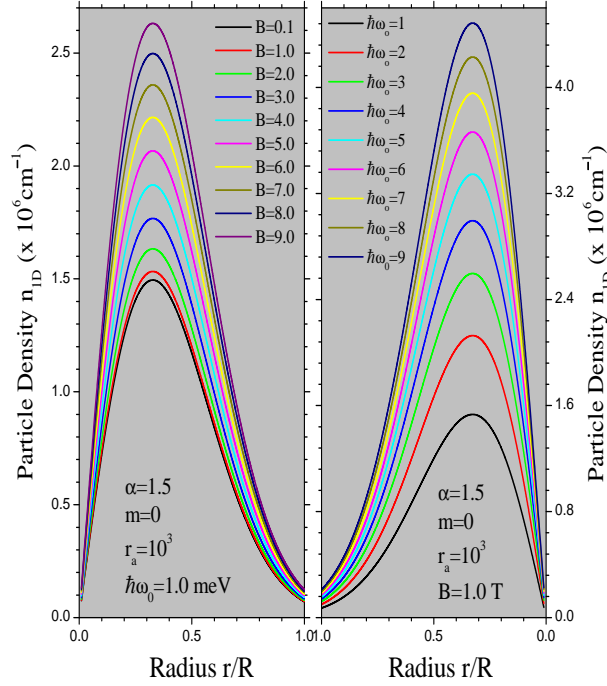


FIG. 12: (Color online) The particle density n_{1D} as a function of the reduced radius r/R for the several values of the magnetic field (left panel) and confinement potential (right panel). The parameters are as listed inside the picture. Again, it is a GaAs/Ga_{1-x}Al_xAs quantum wire. [After Kushwaha, Ref. 39].

the electronic excitation spectrum happens to be so very intricate [see Fig. 11], the Fermi energy will not be a smooth function of the magnetic field (or flux). This intricacy should also lead to complex structures in the magneto-transport phenomena.

Figure 13 depicts the current density as a function of the reduced radius for several values of the magnetic field. The parameters used are: the confinement potential $\hbar\omega_0 = 1.0$ meV, aspect ratio $r_a = 1000$, $\alpha = 1.5$, and $kz = 1.8^\circ$. Other material parameters are the same as before. We observe that the larger the magnetic field, the greater the current density. This is what we should expect intuitively: the larger the magnetic field, the stronger the confinement of the charge carriers near the axis and hence greater the current density. The most important aspect this figure reveals is that there is a maximum in the current density and this maximum is again defined exactly by $r/R = 0.3271$. In a certain way, Fig. 12 substantiates the features observed in Fig. 13. This tells us that in a quantum wire the maximum of charge density lies at $r/R = 0.3271$ instead of exactly at the axis. Note that the classical pinch effect in conventional (3D) SSP [6-19] does not share any such feature. Very close to the axis and to the surface of the quantum wire, the minimum of the current density is smallest but still nonzero. Traditionally, θ -pinches ($\Rightarrow J_\theta$) tend to resist the plasma instabilities due to the famous *frozen-in-flux* theorem (see Appendix B) [47], whereas z -pinches ($\Rightarrow J_z$) tend to favor the confinement phenomena. The magnitude of J_z is double of that of the J_θ just as dictated by Eqs. (13). We believe that these currents are of

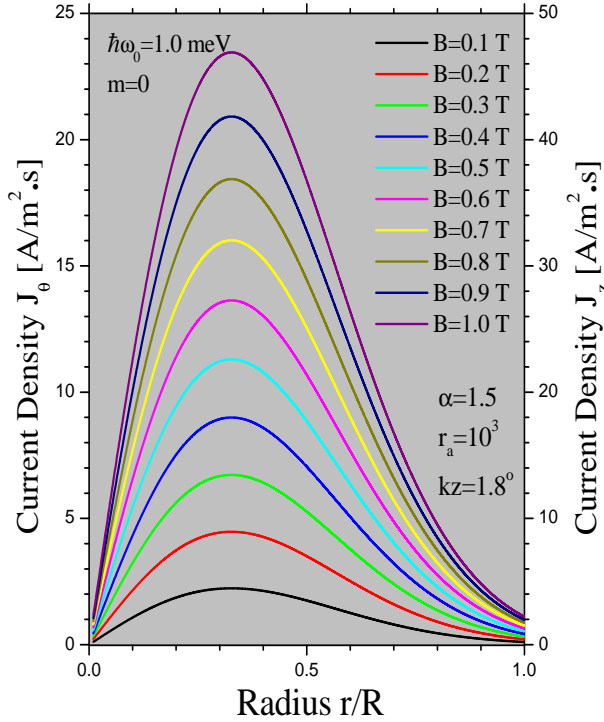


FIG. 13: (Color online) The current density J_θ (J_z) on the left (right) vertical axis vs. the reduced radius r/R for the several values of the magnetic field. The parameters used are: $\hbar\omega_0 = 1.0$ meV, aspect ratio $r_a = 1000$, $\alpha = 1.5$, and $kz = 1.8^\circ$. For a GaAs/Ga_{1-x}Al_xAs quantum wire just as before. [After Kushwaha, Ref. 39].

moderate strength and would not cause an undue heating of the two-component plasma in the quantum wires which are generally subjected to experimental observations at low temperatures.

There are several other interesting and important issues such as the equilibrium, temperature, recombination, and population inversion the consideration of which would certainly give a better insight into the problem. The determination of the radial velocity and the pinch radius as a function of time, after the inception of the pinch, should be significant. The aspect of population inversion enabling the magnetized quantum wires to act as optical amplifiers has recently been discussed in a different context [48-50]. These issues are deferred to a future publication.

III. CONCLUDING REMARKS

In summary, we have investigated the quantum analogue of the classical pinch effect in finite quantum wires with cylindrical symmetry. Since the late 1940s the pinch effect in a gas discharge has been investigated intensively in laboratories throughout the world, because it offers the possibility of achieving the magnetic confinement of a hot plasma (a highly ionized gas) necessary for the successful operation of a thermonuclear or fusion reactor. In solid state plasmas the issues related to confinement, as discussed above, are not encountered. However, since no system provides an ideal environment in

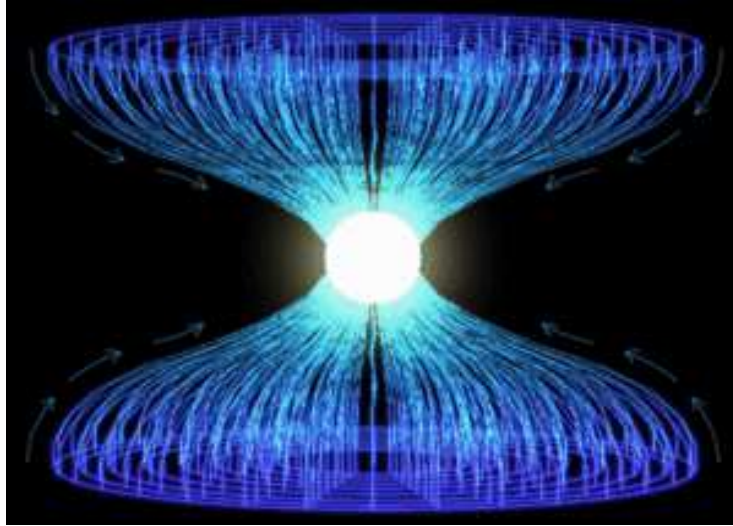


FIG. 14: (Color online) Despite the varied views about its shape, size, and life, the radiating sphere of the sun is known to be the best example of the Birkeland currents focusing into a z-pinch plasma. The result is a spherically focused and illuminating matter in the center of the solar system: the misunderstood sun.

the real world, the SSPs also pose challenges. In a conventional SSP with no impurities, the thermally excited pair density is a function of temperature only. Any deviation from this (thermal) equilibrium can (and, generally, does) give rise to recombination, which, in turn, affects the pinching process. The desired maintenance of the equilibrium pair density occurs through various processes such as Coulomb interactions and particle-lattice interactions, which are not independent and hence cause unintended consequences. The quantum wires – just as other low-dimensional structures such as quantum wells and quantum dots – are the systems in which most of the experiments are performed at low (close to zero) temperatures. Therefore, the risks of thermal non-equilibrium and recombination are much smaller than those ordinarily encountered in conventional SSP. This implies that two-component quantum wires at low temperatures offer an ideal platform for the realization of the quantum pinch effects.

Myriad of applications of quantum pinches bud out from the very thought of the self-focused, two-component plasma in a quantum wire with cylindrical symmetry. The plasma by definition is electrically conductive implying that it responds strongly to electromagnetic fields. The self-focusing (or pinching) only adds to the response. The quantum wire brings all this to the nanoscale. Therefore, we are designing an electronic device that can (and will) control the particle beams at the nanoscale. Potential applications include extremely refined nanoswitches, nanoantennas, optical amplifiers, and precise particle-beam nanoweapons, just to name a few. The greatest advantage of the quantum pinch effect over its classical counterpart is that it offers a Gaussian-like cycle of operation with two minima passing through a maximum. The smooth functionality of the plasma devices is, however, based on a single tenet: there must be means not only to produce it, but also to sustain it.

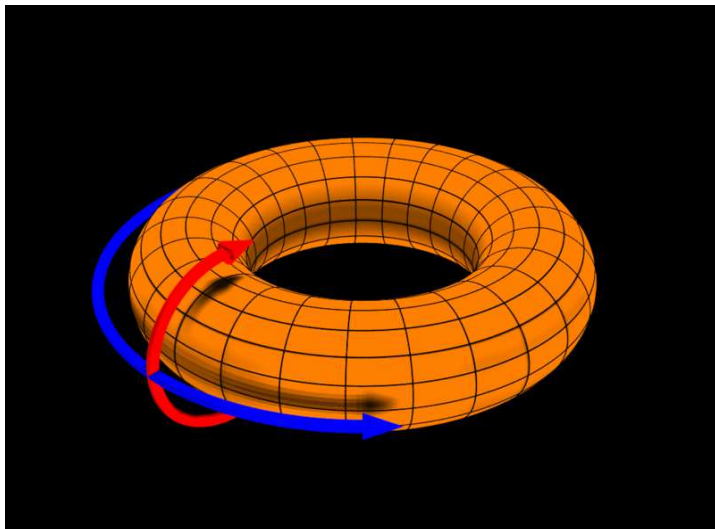


FIG. 15: (Color online) A toroidal tube depicting the poloidal (θ) direction [red arrow] and the toroidal (ϕ) direction [blue arrow]. Notably absent is the radial coordinate which starts from the center of the tube and points out. Nothing is perfect: this torus breaks the θ symmetry. [After Dave Burke (2006)].

According to one retelling, Prometheus – the (mythological) Greek God – gave mankind not just the fire but the very arts of civilization itself - from writing to medicine to astronomy. Fusion is the Promethean fire that has lit the heavens for billions of years. It is the ultimate clean, renewable energy resource, burning seawater as fuel, and producing no carbon dioxide, smoke, or radioactive waste. What it does produce is a prodigious and inexhaustible source of energy - in principle, a teaspoon of hydrogen can generate as much energy as 10 metric tons of coal. Fusion - it powers the Sun; it powers the Stars; it powers the Galaxy. Why can we not make it power the Earth as well?

Acknowledgments

The author feels grateful to Loren N. Pfeiffer who affirmed the feasibility of achieving the aspect ratio of $r_a = 1000$ in the semiconducting quantum wires within the current technology and for the fruitful discussions. He would also like to express his sincere thanks to Alex Maradudin, Allan MacDonald, Bahram Djafari, H. Sakaki, Bob Camley, Jun Kono, Naomi Halas, Peter Nordlander, and Chizuko Dutta for useful communications and stimulating discussions on various aspects related to the subject. He is appreciative of Kevin Singh for the invaluable help with the software during the course of this investigation. Finally, he should like to thank Dr. K.K. Phua, Editor-in-Chief, for the invitation to contribute to this subject, which is still in its infancy, and for his great patience.

Appendix A: The Equilibrium Analysis of The Pinch Geometries

1. One Dimension

One dimensional geometry is generally a cylindrical tube which is symmetrical in the axial (z) direction as well as in the azimuthal (θ) direction. Three pinch geometries generally studied in one dimension are: the θ -pinch, the Z-pinch, and the screw pinch. The one-dimensional pinches are known after the direction in which the current flows. Note that we assume the physical geometry to be made up of non-magnetic materials, which implies $\mathbf{B} \equiv \mathbf{H}$ in the Maxwell equations. Also, we restrict ourselves to the situation shielded by $\nabla \cdot \mathbf{J} = 0$, i.e., where we discard the displacement current in the fourth Maxwell equation. In addition, the magnetic field \mathbf{B} is only the function of r , i.e., $\mathbf{B} = B_z(r)\hat{z} + B_\theta(r)\hat{\theta}$.

a. The θ -pinch

The θ -pinch has a magnetic field oriented in the z direction [i.e., $\mathbf{B} = B_z(r)\hat{z}$]. Then employing Ampere's law yields

$$\frac{1}{c} \mathbf{J} = \frac{1}{4\pi} (\nabla \times \mathbf{B}) = \frac{1}{4\pi r} \frac{d}{d\theta} B_z(r) \hat{r} - \frac{1}{4\pi} \frac{d}{dr} B_z(r) \hat{\theta} \quad (\text{A1})$$

Knowing that \mathbf{B} is only a function of r , this simplifies to

$$\frac{1}{c} \mathbf{J} = -\frac{1}{4\pi} \frac{d}{dr} B_z(r) \hat{\theta} \quad (\text{A2})$$

So, \mathbf{J} points in the θ direction. Thus, the equilibrium condition $[\nabla p = \frac{1}{c} (\mathbf{J} \times \mathbf{B})]$ reads:

$$\frac{d}{dr} \left(p + \frac{1}{8\pi} B_z^2 \right) = 0 \quad (\text{A3})$$

Symbol p refers to the kinetic pressure of the plasma. Notice that the θ -pinch tends to resist the plasma instabilities. This is due in part to the Alfvén's theorem (or frozen-in-flux theorem) [see Appendix B].

b. The Z-pinch

The Z-pinch has a magnetic field oriented in the θ direction [i.e., $\mathbf{B} = B_\theta(r)\hat{\theta}$]. Again, employing Ampere's law yields

$$\frac{1}{c} \mathbf{J} = \frac{1}{4\pi} (\nabla \times \mathbf{B}) = \frac{1}{4\pi r} \frac{d}{dr} (r B_\theta(r)) \hat{z} - \frac{1}{4\pi} \frac{d}{dz} B_\theta(r) \hat{r} \quad (\text{A4})$$

Since \mathbf{B} is only a function of r , this reduces to

$$\frac{1}{c} \mathbf{J} = \frac{1}{4\pi r} \frac{d}{dr} (r B_\theta(r)) \hat{z} \quad (\text{A5})$$

So, \mathbf{J} points in the z direction. Thus, the equilibrium condition $[\nabla p = \frac{1}{c} (\mathbf{J} \times \mathbf{B})]$ reads:

$$\frac{d}{dr} \left(p + \frac{1}{8\pi} B_\theta^2 \right) + \frac{1}{4\pi r} B_\theta^2 = 0 \quad (\text{A6})$$

Since particles in the plasma basically follow the magnetic field lines, the Z-pinch leads them around in circles. Therefore, the Z-pinch offers excellent confinement characteristics [see Fig. 14].

c. The screw pinch

In the screw pinch, the magnetic field has a θ component as well as a z component [i.e., $\mathbf{B} = B_z(r)\hat{z} + B_\theta(r)\hat{\theta}$]. The screw pinch is explicitly an effort to merge the stability aspects of the θ -pinch and the confinement aspects of the Z-pinch. Referring once again to Ampere's law

$$\frac{1}{c} \mathbf{J} = \frac{1}{4\pi} (\nabla \times \mathbf{B}) = \frac{1}{4\pi r} \frac{d}{dr} (r B_\theta(r)) \hat{z} - \frac{1}{4\pi} \frac{d}{dr} B_z(r) \hat{\theta} \quad (\text{A7})$$

So, this time, \mathbf{J} has a component in the z direction and a component in the θ direction. Thus, the equilibrium condition $[\nabla p = \frac{1}{c} (\mathbf{J} \times \mathbf{B})]$ reads:

$$\frac{d}{dr} \left(p + \frac{1}{8\pi} (B_z^2 + B_\theta^2) \right) + \frac{1}{4\pi r} B_\theta^2 = 0 \quad (\text{A8})$$

It is noteworthy that with the neglect of the displacement current in the fourth Maxwell equation, it is quite appropriate to ignore Coulomb's law as well. This is because the electric field is completely determined by the curl equations and Ohm's law $[\mathbf{J} = \sigma \mathbf{E}]$. If the displacement current is retained and $\nabla \cdot \mathbf{E} = 4\pi\rho_e$ is taken into account, corrections of only the order of v^2/c^2 result. For the normal MHD problems these are completely negligible. That is to say that the whole analysis in this Appendix lies within the legitimate realm of MHD.

2. Two Dimensions

A common problem with one-dimensional pinches is the end losses. Most of the motion of particles is along the magnetic field. With the θ -pinch and the screw-pinch, this leads particles out of the end of the machine very quickly, resulting in a loss of mass and energy. Besides, the Z-pinch has severe instability problems. Though particles can be reflected to some extent with magnetic mirrors, even these allow considerable number of them to still pass through. A common remedy of controlling these end losses is to bend the cylinder around into a torus [see Fig. 15]. Unfortunately, this breaks θ symmetry, as paths on the inner portion of the torus are shorter than the those on the outer portion. Thus a new theoretical framework is needed. This gives rise to the famous Grad-Shafranov equation numerical solutions of which have yielded some equilibria, most notably that of the reversed pinch.

Appendix B: Alfvén's Frozen-in-Flux Theorem

For the plasma assumed to be a perfect conductor [with the conductivity $\sigma \rightarrow \infty$], the Ohm's law renders:

$$E + \frac{1}{c} (\mathbf{V} \times \mathbf{B}) = 0 \quad (\text{B1})$$

This is sometimes referred to as the flux freezing equation. The nomenclature comes about because Eq. (B1) implies that the magnetic flux through any closed contour in the plasma, each element of which moves with the local velocity, is a conserved quantity. In order to verify this assertion, let us consider the magnetic flux ϕ_m , through a contour C , which is co-moving with the plasma:

$$\phi_m = \int_S \mathbf{B} \cdot d\mathbf{S}, \quad (\text{B2})$$

where \mathbf{S} is some surface which spans \mathbf{C} . The time rate of change of ϕ_m is made up of two parts. First, there is the part due to the time variation of \mathbf{B} over the surface \mathbf{S} . This can be written as

$$\left. \frac{\partial \phi_m}{\partial t} \right|_1 = \int_S \frac{\partial \mathbf{B}}{\partial t} \cdot d\mathbf{S} \quad (\text{B3})$$

Using the third curl Maxwell equation, this becomes

$$\left. \frac{\partial \phi_m}{\partial t} \right|_1 = -c \int_S (\nabla \times \mathbf{E}) \cdot d\mathbf{S} \quad (\text{B4})$$

Second, there is the part due to the motion of \mathbf{C} . If $d\mathbf{l}$ is an element of \mathbf{C} , then $\mathbf{V} \times d\mathbf{l}$ is the area swept out by $d\mathbf{l}$ per unit time. Hence the flux crossing this area is $\mathbf{B} \cdot (\mathbf{V} \times d\mathbf{l})$. It follows that

$$\left. \frac{\partial \phi_m}{\partial t} \right|_2 = \int_C \mathbf{B} \cdot (\mathbf{V} \times d\mathbf{l}) = \int_C (\mathbf{B} \times \mathbf{V}) \cdot d\mathbf{l} \quad (\text{B5})$$

Using Stokes' theorem, this becomes

$$\left. \frac{\partial \phi_m}{\partial t} \right|_2 = - \int_S \nabla \times (\mathbf{B} \times \mathbf{V}) \cdot d\mathbf{S} \quad (\text{B6})$$

Hence, the total time rate of change of ϕ_m is given by, from Eqs. (B4) and (B6),

$$\frac{d\phi_m}{dt} = -c \int_S \nabla \times \left[\mathbf{E} + \frac{1}{c} (\mathbf{V} \times \mathbf{B}) \right] \cdot d\mathbf{S} \quad (\text{B7})$$

Given the condition in Eq. (B1), Eq. (B7) is led to conclude that

$$\frac{d\phi_m}{dt} = 0 \quad (\text{B8})$$

In other words, ϕ_m remains constant in time for an arbitrary contour. This, in turn, implies that the magnetic field-lines must move with the plasma. That is to say that the field-lines are frozen into the plasma. Since the magnetic field-lines can be regarded as infinitely thin flux-tubes, we conclude that MHD plasma motion also maintains the integrity of field-lines. That means magnetic field-lines embedded in an MHD plasma can never break and reconnect: i.e., MHD forbids any change in the topology of the field-lines. It turns out that this is an extremely restrictive constraint.

-
- [1] J.A. Pollock and S. Barraclough, Proc. Roy. Soc. (New South Wales) **39**, 131 (1905).
 - [2] E.F. Northrup, Phys. Rev. **24**, 474 (1907).
 - [3] W.H. Bennett, Phys. Rev. **45**, 890 (1934).
 - [4] L. Tonks, Trans. Trans. Electrochem. Soc. **72**, 167 (1937).
 - [5] G.P. Thompson and M. Blackman, British Patent **817681** (1946).
 - [6] M. Glicksman and M. C. Steele, Phys. Rev. Lett. **2**, 461 (1959).
 - [7] M. Glicksman and R.A. Powlus, Phys. Rev. **121**, 1659 (1961).
 - [8] A.G. Chynoweth and A.A. Murray, Phys. Rev. **123**, 515 (1961).
 - [9] B. Ancker-Johnson and J.E. Drummond, Phys. Rev. **131**, 1961 (1963); **132**, 2372 (1963).
 - [10] M. Toda and M. Glicksman, Phys. Rev. **140**, A1317 (1965).
 - [11] K. Ando, J. Phys. Soc. Japan **21**, 1295 (1966).
 - [12] K. Hubner and L. Blossfeld, Phys. Rev. Lett. **19**, 1282 (1967).
 - [13] K. Ando and M. Glicksman, Phys. Rev. **154**, 316 (1967).
 - [14] K. S. Thomas, Phys. Rev. Lett. **23**, 746 (1969).
 - [15] W.S. Chen and B. Ancker-Johnson, Phys. Rev. B **2**, 4477 (1970).
 - [16] M. Glicksman, Jap. J. Appl. Phys. **3**, 354 (1964).
 - [17] H. Schmidt, Phys. Rev. **149**, 564 (1966).
 - [18] B.V. Paranjape, J. Phys. Soc. Jpn. **22**, 144 (1967).
 - [19] W.S. Chen and B. Ancker-Johnson, Phys. Rev. B **2**, 4468 (1970).
 - [20] K.v. Klitzing, G. Dorda, and M. Pepper, Phys. Rev. Lett. **45**, 494 (1980).
 - [21] D.C. Tsui, H.L. Stormer, and A.C. Gossard, Phys. Rev. Lett. **48**, 1559 (1982).
 - [22] M.S. Kushwaha and F. Garcia-Moliner, Phys. Lett. A **205**, 217 (1995).
 - [23] M.S. Kushwaha and P. Zielinski, Solid State Commun. **112**, 605 (1999).
 - [24] For an extensive review of electronic, optical, and transport phenomena in the systems of reduced dimensions, such as quantum wells, quantum wires, quantum dots, and (electrically/magnetically) modulated 2DEG, see M.S. Kushwaha, Surf. Sci. Rep. **41**, 1 (2001).
 - [25] M.S. Kushwaha and H. Sakaki, Phys. Rev. B **69**, 155331 (2004).
 - [26] M.S. Kushwaha and H. Sakaki, Solid State Commun. **130**, 717 (2004).
 - [27] M.S. Kushwaha, Phys. Rev. B **77**, 241305(R) (2008).
 - [28] M.S. Kushwaha and S.E. Ulloa, Phys. Rev. B **73**, 205306 (2006).
 - [29] M.S. Kushwaha and S.E. Ulloa, Phys. Rev. B **73**, 045335 (2006).
 - [30] M.S. Kushwaha, Phys. Rev. B **74**, 045304 (2006).
 - [31] M.S. Kushwaha, Phys. Rev. B **76**, 245315 (2007).
 - [32] M.S. Kushwaha, J. Appl. Phys. **104**, 083714 (2008).
 - [33] M.S. Kushwaha, J. Appl. Phys. **106**, 066102(C) (2009).
 - [34] M.S. Kushwaha, J. Chem. Phys. **135**, 124704 (2011).

- [35] M.S. Kushwaha, AIP Advances **2**, 032104 (2012).
- [36] M.S. Kushwaha, AIP Advances **3**, 042103 (2013);
- [37] M.S. Kushwaha, Electronics Letters **50**, 1305 (2014).
- [38] M.S. Kushwaha, AIP Advances **4**, 127151 (2014).
- [39] M.S. Kushwaha, Appl. Phys. Lett. **103**, 173116 (2013).
- [40] B. Tanatar, Solid State Commun. **92**, 699 (1994).
- [41] J.S. Thakur and D. Neilson, Phys. Rev. B **56**, 4671 (1997).
- [42] S. Das Sarma and E.H. Hwang, Phys. Rev. B **59**, 10730 (1999).
- [43] L.J. Slater, *Confluent Hypergeometric functions* (Cambridge, London, 1960).
- [44] M. Abramowitz and I.A. Stegun, *Handbook of Mathematical Functions* (Dover, New York, 1972).
- [45] J. Spanier and K.B. Oldham, *An Atlas of Functions* (Springer-Verlag, Berlin, 1987).
- [46] L.N. Pfeiffer, Private Communication (2013).
- [47] H. Alfvén, Arkiv foer Matematik, Astronomi, och Fysik **39**, 2 (1943).
- [48] M.S. Kushwaha, Phys. Rev. B **78**, 153306 (2008).
- [49] M.S. Kushwaha, J. Appl. Phys. **109**, 106102(C) (2011).
- [50] M.S. Kushwaha, Mod. Phys. Lett. B **28**, 1430013 (2014).